The partition sum of methane at high temperature

Christian Wenger, Jean-Paul Champion, Vincent Boudon

The partition sum of methane at high temperature

C. Wenger, J.P. Champion and V. Boudon
Institut Carnot de Bourgogne - UMR 5209 CNRS–Université de Bourgogne,
9, av. Alain Savary, B.P. 47870, F-21078 Dijon Cedex, France.

June 24, 2008

Abstract

The total internal partition function of methane is revisited to provide reliable values at high temperature. A multi-resolution approach is used to perform a direct summation over all the rovibrational energy levels up to the dissociation limit. A computer code is executable on line at the URL : http://icb.u-bourgogne.fr/JSP/TIPS.jsp to allow the calculation of the partition sum of methane at temperatures up to 3000 K. It also provides detailed information on the density of states in the relevant spectral ranges. The recommended values include uncertainty estimates. It is shown that at the upper limit of 3000 K, the systematic error (underestimation) of previous calculations (HITRAN 2004) reaches −50% equivalent to a temperature error of the order of +200 K.

Keywords : Partition sum; Methane; Computational spectroscopy; Rovibrational spectroscopy; Spectroscopic databases

1 Introduction

Methane plays a major role in the atmospheres of a number of astrophysical objects at temperatures up to around 3000 K (see for instance [1, 2, 3]). Predicting high temperature spectra, needed to understand the physical chemistry of these objects, implies accurate modelling of highly excited states as well as transition intensities including hot bands. Deriving reliable values of the partition function represents one of the multiple aspects of such a challenge. At present, due to the complexity of the modelling of spherical top spectra, the calculation of the total internal partition function of methane relies on the basic harmonic oscillator and quasi-rigid rotor approximations. For instance, the most recent reviews on the partition functions of various molecular species [4, 5] have promoted the generalized use of the analytical formulae of McDowell [6] for spherical tops. Furthermore, the HITRAN 2004 molecular spectroscopic database [7] includes data tables extrapolating these formulae up to 3000 K, whereas the above approximations are valid up to around 1000 K only. Recent calculations of converged rovibrational energies have been reported in Ref. [8]. They were also focused in the temperature range of $100 - 1000$ K and the proposed separable-rotation appoximation is accurate within 2% only in this range.The present work was motivated by the need for reliable values in recent investigations on the high temperature emission spectrum of methane [9].

Following the Boltzmann distribution at thermodynamic equilibrium, the contribution to the partition sum of the subsequent layers of energy levels in any molecular system drastically depend on temperature. Typically, for the methane molecule, at 2500 K the maximum contribution is around 10 000 cm^{-1}. Unfortunately, this spectral region is far from being exhaustively modelled at high resolution. On the other hand, it is obvious from the knowledge of the lower polyads of the molecule [10, 11] that the harmonic oscillator approximation becomes qualitatively and quantitatively unrealistic. Furthermore, at this temperature, the contribution of higher energy levels cannot be neglected up to around 35 000 cm^{-1} which is not far from the dissociation limit of methane. Consequently, an exhaustive and realistic modelling of the full energy spectrum of the molecule is required to get reliable values of the partition function up to 3000 K.

The present work was based on a multi-resolution approach to perform a direct summation over all the rovibrational levels up to the dissociation limit. The partition sum $Q(T)$ is formally expressed as

$$Q(T) = \sum_{i=\text{all states}} \exp\left(\frac{-E_i}{kT}\right) = \sum_{j=\text{all levels}} g_j \exp\left(\frac{-E_j}{kT}\right) \quad (1)$$

where g_j denotes the total degeneracy of the E_j *levels*, *i. e.* the number of all possible *states* E_i including electronic, vibrational and rotational degrees of freedom. Three sets of levels were considered in the energy spectrum of methane. In the lower energy set, high-resolution modelling of the individual rovibrational energy

levels was performed. In the upper two sets, lower-resolution descriptions based on statistical considerations were applied.

The theoretical details are developped in the next section. The subsequent section describes the computer implementation of the method. Several physical approximations, including the basic harmonic oscillator and rigid rotor approximation were investigated for comparison and validation purposes. The last section is devoted to quantitative estimates of the accuracy of the calculations as a function of temperature.

2 Theoretical model

The extremely large density of states in the higher-energy layers makes it impossible to model the rovibrational energy levels individually. The model developed in the present work combines, in a consistent way, individual and statistical quantum descriptions of the methane spectrum. The lower layers of the energy spectrum are described through the well-proven effective Hamiltonian global approach [12, 10, 11]. The higher-energy layers are extrapolated and statistically modelled on the basis of appropriate physical approximations. Three sets of levels are considered according to

$$Q(T) = \sum_{i=\text{indiv levels}} g_i \exp\left(\frac{-E_i^{STDS}}{kT}\right) + \sum_{j=\text{stat levels}} G_j \exp\left(\frac{-E_j^{Rot\ Extra}}{kT}\right) + \sum_{k=\text{stat levels}} G_k \exp\left(\frac{-E_k^{Morse}}{kT}\right). \quad (2)$$

Following the polyad pattern of methane, all the energy levels (individual or statistical) are labeled by the polyad number p defined as

$$p = 2v_1 + v_2 + 2v_3 + v_4, \quad (3)$$

where the v_i are the vibrational quantum numbers associated to the four normal modes of the molecule, and by the rotational quantum number J. The total degeneracy g_i of the individual levels is derived from spin statistics

$$g_i = (2J+1)d_s \quad (4)$$

where d_s = 5, 5, 2, 3 and 3 for the A_1, A_2, E, F_1 and F_2 rovibrational species respectively. It gathers the weights 5, 0, 1, 0, 3 of odd parity levels and the weights 0, 5, 1, 3, 0 of even parity levels, knowing that the symmetry of the nuclear spin function of $^{12}CH_4$ is $5A_1 + E + 3F_2$ (see Ref. [13] for detailed discussions of the classification of energy levels for polyatomic molecules). The calculation of the three sums in $Q(T)$ is detailed in sections 2.1, 2.2 and 2.3. The calculation of the global degeneracies G_j and G_k of the statistical levels is detailed in section 2.4.

2.1 Individual levels from the lower polyads

The lower levels were calculated individually using a unique rovibrational effective Hamiltonian implemented in the STDS package [14]. They include the rovibrational levels fitted to high-resolution experimental data for the lower five polyads : Ground State, Dyad, Pentad, Octad, Tetradecad (see [11, 15]) as well as extrapolated levels up to a value J_{max} of J fixed pragmatically to keep the calculation within a reasonable use of computational resources. They include as well the predicted $J = 0$ levels of the subsequent polyads $p = 6$ to 9. Three models corresponding to various orders of approximation have been considered (see Table 1).

The zero order corresponds to the usual harmonic oscillator and rigid rotor approximation. It was used to validate our computer code by reproducing the alternative original calculation of McDowell [6]. Other test calculations performed at the second order of approximation and at the highest order presently available for the lower four polyads [15] - denoted as best in Table 1 - proved to be quite comparable. In fact, a second order expansion was found to realize the best compromise regarding both accuracy and extrapolation reliability. The corresponding second order parameters were those reported in [16]. Note that they were derived from a second order fit of experimental data and not from truncation to the second order of a higher order fit. The root mean square deviation of this second order fit was of the order of 1 cm^{-1} over the full range of presently assigned lower-polyad experimental data. The corresponding characteristics of the polyads are given in Table 2 . For the calculation of $E_{mean}(p)$ all the vibrational sublevels were given the same weight independently of their

Table 1: Characteristics of the effective hamiltonian global description of the lower polyads

			Hamiltonian Order		
Polyad Number	*Polyad Name*	J_{max}	*0*	*2*	*best*
0	Ground State	60	0	2	6
1	Dyad	50	0	2	6
2	Pentad	40	0	2	4
3	Octad	30	0	2	4
4	Tetradecad	20	0	2	4
5	Icosad	10	0	2	2
6	Triacontad	0	0	2	2
7	Tetracontad	0	0	2	2
8	Pentacontakaipentad	0	0	2	2
9	Heptacontad	0	0	2	2

symmetry species. Note that E_{mean} is systematically larger than the middle energy $(E_{max}(p) + E_{min}(p))/2$ reflecting the polyad specificity of methane. The values $E_c(p, J = 0)$ refer to the zero point energy of the Morse function for direct comparison with the values quoted in Table 3. The corresponding diagram is plotted in the bottom panel of Figure 1.

The uncertainty of the predicted levels in the present work is estimated to range from 1 to 10 cm^{-1} or more in the case of faraway extrapolated levels (section below). However, in contrast with the zero order approximation, the main rovibrational couplings (Fermi, Coriolis, Darling Dennison, ...) and thus the anharmonicity effects are explicitely taken into account in our model.

Table 2: Lower polyad characteristics (second order STDS prediction)

(1)	(2)	(3)	(4)	(5)	(6)	(7)
p	$N_{vib}(p)$	$E_{\min}(p)$	$E_{\max}(p)$	$E_{\mathrm{mean}}(p)$	$E_c(p, J = 0)$	*Spin Sum*
0	1	0.0	0.0	0.0	710.9	5
1	2	1310.1	1533.6	1421.9	2132.8	5
2	9	2587.1	3065.5	2840.9	3551.8	31
3	24	3870.3	4595.8	4265.3	4976.2	79
4	60	5121.3	6124.4	5681.1	6392.0	192
5	134	6375.7	7651.3	7097.0	7807.9	432
6	280	7599.7	9176.5	8500.9	9211.8	904
7	538	8823.7	10700.1	9901.3	10612.2	1720
8	996	10019.8	12221.9	11293.7	12004.6	3198
9	1746	11212.4	13742.1	12680.5	13391.4	5598

$N_{\mathrm{vib}}(p)$ is the number of vibrational sublevels in polyad p. All wavenumbers in cm^{-1}.

2.2 Rotationally extrapolated statistical levels from the lower polyads

The second set of levels in Eq. 2 consists of statistical rovibrational levels of the previous polyads rotationally extrapolated up to the dissociation limit (and in any case $J \leq 100$). We applied the following simple procedure. For each polyad p $(0 \leq p \leq 9)$, the rotational fine structure for $J = J_{\max}$, predicted using STDS (Table 1), was considered as a reference pattern for the higher J rotational fine structures and duplicated after shifting and scalling to account statistically for the above mentioned rovibrational couplings. It can be formally expressed as

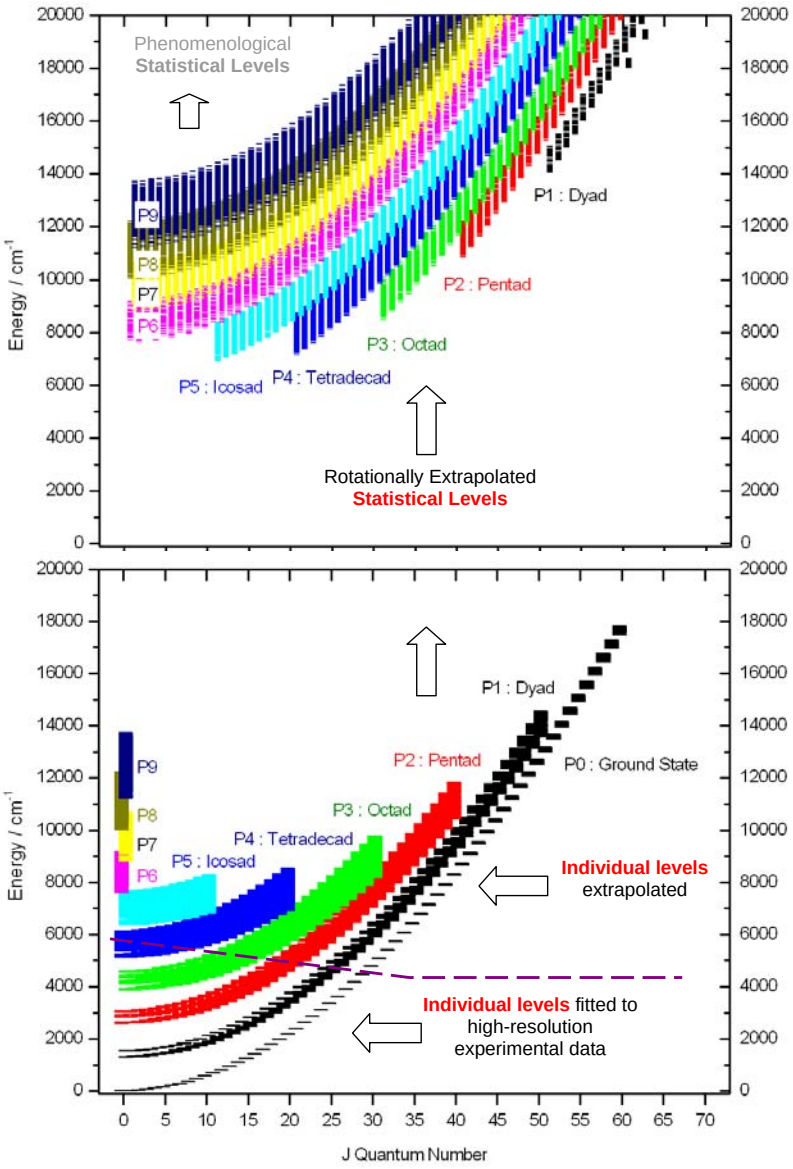

Figure 1: Schematic Energy Diagram showing the three sets of rovibrational levels included in the model. The so-called phenomenological statistical levels extend up to the dissociation limit ste to 37 000 cm^{-1}

$$\widetilde{E}_i(p,J) = \widetilde{E}_c(p,J) + (E_i(p,J_{\max}) - E_c(p,J_{\max})) \times \frac{\widetilde{E}_w(p,J)}{E_w(p,J_{\max})} \quad (5)$$
$$\text{for} \quad J > J_{\max} \quad \text{and} \quad i = 1,...,N_{rv}(p,J_{\max}).$$

In this equation $\sim$ denotes quantities statistically estimated. $N_{rv}(p,J_{\max})$ is the exact number of rovibrational levels for polyad p at $J = J_{\max}$. The rotational structure centers $\widetilde{E}_c(p,J)$ for $J > J_{\max}$ were calculated according to the quasi-rigid rotor approximation

$$\widetilde{E}_c(p,J) = E_c(p,J=0) + B_0 J(J+1) - D_0 J^2(J+1)^2 \quad (6)$$

where B_0 and D_0 denote respectively the inertia and the centrifugal distortion constants.

The rotational structure widths $\widetilde{E}_w(p,J)$ for $J > J_{\max}$ were set assuming a linear dependency of Coriolis effects with J as justified by the matrix elements of the leading terms

$$\widetilde{E}_w(p,J) = E_w(p,J=0) \times F_{Coriolis} \times J \quad (7)$$

where the Coriolis expansion factor $F_{Coriolis}$ was set to 0.03 as determined from the statistical behaviour observed on the lower polyads. Finally $E_c(p, J = 0)$ and $E_w(p, J = 0) = E_{max}(p) - E_{min}(p)$ are the centers and widths as predicted from our STDS model (Table 2).

2.3 Phenomenological statistical levels from the upper polyads

The remaining higher excited levels were modelled using a statistical approach consistent with the observed behaviour of the lower polyads. Several statistical studies have been devoted to molecular systems mainly focused on the subject of chaos. In particular, the density of levels in vibrational spectra of molecules has been investigated yielding analytical expressions for the spectral density moments of systems of N coupled Morse oscillators (see [17]). However these works are not directly suitable for the statistical description of the rotational fine structure of methane polyads where strong bend-stretch interactions are involved. We have thus followed a phenomenological approach for the third set of levels in Eq. 2. It consists of statistical rovibrational levels vibrationally and rotationally extrapolated to polyads $p = 10$ and higher up to the dissociation limit. The vibrational structure of these higher polyads was modelled in the frame of the Morse potential yielding the vibrational energies

$$E(v) = \omega(v + 1/2) - \frac{\omega^2}{4D}(v + 1/2)^2. \tag{8}$$

In our model this expression, normally designed for a single oscillator with vibrational quantum number v, was applied to estimate the polyad centers through the following substitutions : $v \longrightarrow p$: polyad number and $E(v) \longrightarrow E_c(p)$: energy of the center of polyad p. The D parameter of the Morse function (dissociation limit) was set to $\Delta + E_c(0)/2$ where $\Delta = 37\ 000\ \text{cm}^{-1}$ derived from the experimental value of Ref. [18]. The wavenumber of the fundamental level ω and the polyad number p_{lim} at the dissociation limit were then determined by *two boundary conditions*.

- The first one, expressing the continuity between the lower-polyad effective Hamiltonian (STDS) prediction and the Morse expression for higher polyads is written as

$$E_c(p_{\text{sup}}) = \omega(p_{\text{sup}} + 1/2) - \frac{\omega^2}{4D}(p_{\text{sup}} + 1/2)^2 \tag{9}$$

where p_{sup} denotes the number of the upper polyad predicted by STDS ($p_{\text{sup}} = 9$ in our case), and $E_c(p_{\text{sup}})$ the corresponding center energy, yielding

$$\omega = \frac{2D}{(p_{\text{sup}} + 1/2)} \left(1 - \sqrt{1 - \frac{E_c(p_{\text{sup}})}{D}}\right) = 1563.6\ \text{cm}^{-1} \tag{10}$$

- The second one determines p_{lim} from

$$D = E_c(p_{\text{lim}}) = \omega(p_{\text{lim}} + 1/2) - \frac{\omega^2}{4D}(p_{\text{lim}} + 1/2)^2 = \omega\beta - \frac{\omega^2}{4D}\beta^2 \tag{11}$$

where $\beta = p_{\text{lim}} + 1/2$. This equation gives $\beta = 48.24$ and thus p_{lim} was set to 47, the closest integer value satisfying

$$p_{\text{lim}} \simeq \beta - \frac{1}{2}. \tag{12}$$

A schematic diagram of the vibrational polyad centers is represented on Figure 2.

Obviously, the Morse model applied to the vibrational polyads is not directly suitable for the description of the behaviour of the widths of the successive polyads. In fact, we assumed the same dissociation limit for all the vibrational components of the polyads and thus repeated the above procedure for the maximum and minimum energies of the polyads successively. Consistently, we applied similar continuity conditions to the upper and lower limits of polyad $p = 9$ with the corresponding quantities $E_{\text{max}}(9)$ and $E_{\text{min}}(9)$ predicted by

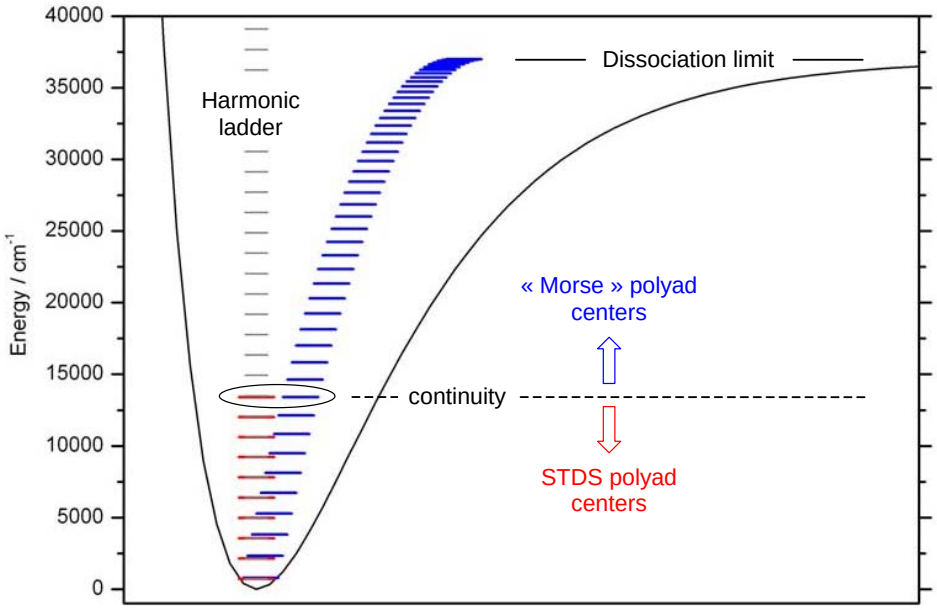

Figure 2: Schematic Energy Diagram showing the vibrational polyad centers. STDS refers to the prediction using the global second order effective Hamiltonian fitted to high-resolution experimental data. From polyad number 10 up to the dissociation limit, polyad centers are calculated using the phenomenological "Morse" approximation.

STDS. Doing so, the widths of the polyads were found to increase with the polyad number up to a maximum value (for $p \sim 24$) and then to decrease until the dissociation limit as quoted in Table 3. Of course, the accuracy of such a model near the dissociation limit is hard to assess. Nevertheless, we believe it gives a description of the level density much more realistic than the harmonic oscillator approximation at intermediate energies relevant for the considered temperature range. Detailed calculations were made to quantify the effect of varying the unique leading Morse parameter D on the partition sums. They were then used to estimate the uncertainty of our results.

All wavenumbers in cm^{-1}. $N(p)$ is the total vibrational degeneracy of polyad p. The corresponding number of vibrational levels is approximately equal to $N(p)/2.4$ (see text). $\widetilde{E}_c(p)$ is the polyad center relative to the Morse minimum energy. $\widetilde{E}_w(p) = \widetilde{E}_{max} - \widetilde{E}_{min}$ is the polyad width.

Finally, on the basis of this modelling of the polyad vibrational structure, a rotational extrapolation was performed applying the same procedure as for the second set of levels (see section 2.2).

2.4 Total degeneracy of the predicted levels

According to the above model, the number of extrapolated statistical levels in the second and third sets in Eq. 2 is equal to the number of levels in reference rotational structure patterns. Consequently, each level represents statistically several invidual levels. In order to account rigorously for the actual total degeneracy (essential for partition sum calculations), each statistical level was affected a degeneracy $G(p, J)$ calculated by

$$G(p, J) = 3.2 \times (2J + 1) \times \frac{N(p)}{N_{\mathrm{stat}}(p)} \tag{13}$$

where $N(p)$ and $N_{\mathrm{stat}}(p)$ denote respectively the exact vibrational degeneracy of polyad p and the corresponding degeneracy of the statistical vibrational levels in the present model with $N_{\mathrm{stat}}(p) = N(p_{\mathrm{sup}})$. The factor $3.2 \times (2J+1)$ holds for the mean total degeneracy of the rovibrational levels including spin statistics and the degeneracy with respect to the magnetic quantum number. The values $N(p)$ were taken from the expression established by Sadovskii *et al* [19] using generating functions and reproduced below,

Table 3: Upper vibrational polyads of methane (Morse extrapolation)

p	$N(p)$	$\widetilde{E}_c(p)$	$\widetilde{E}_w(p)$	p	$N(p)$	$\widetilde{E}_c(p)$	$\widetilde{E}_w(p)$
9	4170	13391.4	2529.7	29	3759720	32021.3	3878.3
10	7061	14630.8	2725.2	30	4705464	32612.4	3804.1
11	11550	15837.8	2907.3	31	5852760	33171.1	3716.5
12	18348	17012.5	3075.8	32	7237461	33697.4	3615.4
13	28380	18154.7	3230.9	33	8900264	34191.3	3500.8
14	42900	19264.4	3372.4	34	10887855	34652.8	3372.8
15	63492	20341.8	3500.5	35	13252899	35081.8	3231.2
16	92234	21386.7	3615.1	36	16055380	35478.5	3076.2
17	131703	22399.3	3716.3	37	19362596	35842.7	2907.7
18	185185	23379.4	3803.9	38	23250700	36174.5	2725.7
19	256684	24327.1	3878.1	39	27804700	36473.9	2530.2
20	351208	25242.4	3938.8	40	33120230	36740.9	2321.3
21	474760	26125.2	3986.0	41	39303550	36975.5	2098.8
22	634712	26975.7	4019.7	42	46473570	37177.6	1862.9
23	839800	27793.7	4039.9	43	54761850	37347.4	1613.5
24	1100580	28579.4	4046.7	44	64314899	37484.7	1350.6
25	1429428	29332.6	4040.0	45	75294180	37589.6	1074.3
26	1841100	30053.4	4019.8	46	87878700	37662.1	784.4
27	2352732	30741.8	3986.1	47	102265020	37702.1	481.1
28	2984519	31397.7	3938.9				

$$N(p) = 24N_{lead}(p) + \frac{1}{2^8}\left(\frac{563}{15}p^4 + \frac{28457}{180}p^3 + \frac{970241}{2520}p^2 + \frac{204347}{420}p + \frac{3797}{16}\right) + \frac{(-1)^p}{2^{10}}\left(\frac{1}{3}p^3 + \frac{13}{2}p^2 + \frac{119}{3}p + \frac{299}{4}\right) \tag{14}$$

with the leading term

$$N_{lead}(p) + \frac{1}{2^{12}\cdot 5}\left(\frac{p^8}{4\cdot 27\cdot 7} + \frac{13p^7}{27\cdot 7} + \frac{3p^6}{2} + \frac{13\cdot 37p^5}{27}\right). \tag{15}$$

The approximate number of vibrational levels of each polyad can be derived from the values quoted in Table 3 by dividing $N(p)$ by the factor 2.4 which represents the asymptotic mean spin statistical weight of the vibrational levels. Due to their statistical character (arising from implicite averaging on both energy and degeneracy), the accuracy of the second and third sets of levels in Eq. 2 is much less than the accuracy of the first set. The uncertainty on energies is hard to estimate rigorously and may be as large as several hundreds of cm^{-1}. However the density and degeneracy of levels at energies relevant for the considered temperature range are more realistic than using the standard harmonic oscillator approximation used so far to evaluate partition sums.

3 Computer code

Our computer code uses as input data a file containing 87 524 rovibrational energy levels of the lower polyads predicted using the second order global effective Hamiltonian [16] implemented in the STDS package [14]. Each record is labeled by the usual indices : the polyad number p, the value of J, the rovibrational symmetry C, a running number α and the corresponding energy E. The quantum numbers J and C are used to derive the degeneracy of the levels. Up to 600 K the statistical levels have no significant contribution so that the summation includes only the primary individual levels contained in the input file (first set in Eq. 2). At higher temperature the program generates the needed higher energy statistical levels and the corresponding global degeneracies according to the model described above.

One of the first test calculations was to reproduce the values of Ref. [6] implemented in HITRAN 2004 [7] by performing a direct summation using our code within the frame of the standard harmonic oscillator and rigid rotor approximation (i.e. zero order of approximation). It turned out that our values from direct summation and the values derived from the McDowell formula [6] agreed within 1% in the full range of temperature from 10 to 3000 K, which represents a good validation of the correct statistical treatment of the level densities and degeneracies for the higher polyads in our model.

A simplified version of our computer code is installed and executable at http://icb.u-bourgogne.fr/JSP/T-IPS.jsp. For any temperature below 3000 K, the program returns the partition sum calculated using the present approach and for comparison the value derived from the McDowell formula [6]. The estimated uncertainty of the present calculation (see section hereafter) is also provided. Useful modeling details about the polyads, the density of levels and the density of quantum states of the molecule are included in downloadable output files (plain text and portable LaTeX formats). The ASCII file containing the input 87 524 rovibrational energy levels mentioned above is also available through the user interface.

Although the present work was focussed on high temperature needs, for completeness towards very low temperature investigations, the separate contributions from the ortho-, meta- and para-methane are given when the direct calculation is based on individual separable levels only (*i. e.* up to 600 K).

4 Results and discussion

The propagation of uncertainties from the rovibrational levels into the partition direct sum depends essentially on the temperature. As mentioned in the preceeding section, up to 600 K, the contribution of statistically extrapolated levels (second and third sets of levels in Eq. 2) is neglegible so that the precision of the corresponding partition sum depends on the precision of the individual levels fitted to high-resolution experimental data only. As mentioned earlier, calculations performed at various orders of approximation do not differ significantly within this temperature range. Even the basic harmonic oscillator approximation gives reliable results. At very low temperatures (below 50 K) similar test calculations revealed no sensible differences between the second order model and higher order models justifying this choice of the second order in all cases.

Of course at higher temperatures (above 1000 K), the contribution of the statistically extrapolated levels increases with temperature so that an important source of uncertainty arises from the unknown modelling error on the highly excited polyads. In fact, the precise knowledge of the individual levels is not absolutely necessary provided that a correct description of the density of states in spectral ranges relevant for each temperature can be achieved. Figure 3 illustrates the impact of the various energy layers to the total partition sum at typical temperatures. It can be seen that at 1000 K the partition sum is fully converged at around 15 000 cm^{-1}. At this temperature, the discrepancy between the densities of levels (and the corresponding densities of quantum states) predicted using the second order anharmonic model and the basic harmonic model is small. The resulting difference between the zero order (HITRAN 2004) and the second order partition sum values is -1.1%. Conversely, at 3000 K the energy levels close to the dissociation limit have a significant contribution to the partition sum. The density of levels above 20 000 cm^{-1} is drastically underestimated using the zero order model and exceeds one order of magnitude above 32 000 cm^{-1}. The resulting difference between the HITRAN 2004 and the present work values reaches -50%. Note that, at this temperature, the zero order direct sum is not fully converged at 37 000 cm^{-1}.

To overcome the lack of theoretical or experimental validation of the modelling of bound states near dissociation we did a series of test calculations by varying the dissociation limit around its experimental value [18]. It turned out that in the less favourable case ($T = 3000$ K), a $\pm 5\%$ variation of the dissociation limit around 37 000 cm^{-1} implied a $\pm 3\%$ variation of the partition direct sum at 3000 K, and only $\pm 1.4\%$ at 2500 K. These values are equivalent to uncertainties on temperatures of the order of $\Delta T = \pm 10$ K and $\Delta T = \pm 4$ K respectively. The above considerations have been used to estimate the precision of the recommended values quoted in Table 4. The number of significant digits was matched to the estimated uncertainty of our calculations. As expected, uncertainties increase rapidely with temperature reflecting the relative contribution of the higher energy levels. They are also converted in terms of temperature uncertainties (column *Equiv.* ΔT of Table 4) since partition functions are often involved in temperature retrieval processes. The values available from HITRAN 2004 (folder *Global Data Files* [7]) are included for comparison. According to our direct calculation uncertainties, systematic errors arising from the harmonic approximation make no doubt in the whole temperature range from 1000 to 3000 K. This is particularly true in the intermediate range from 1000 to 2000 K for which our estimated

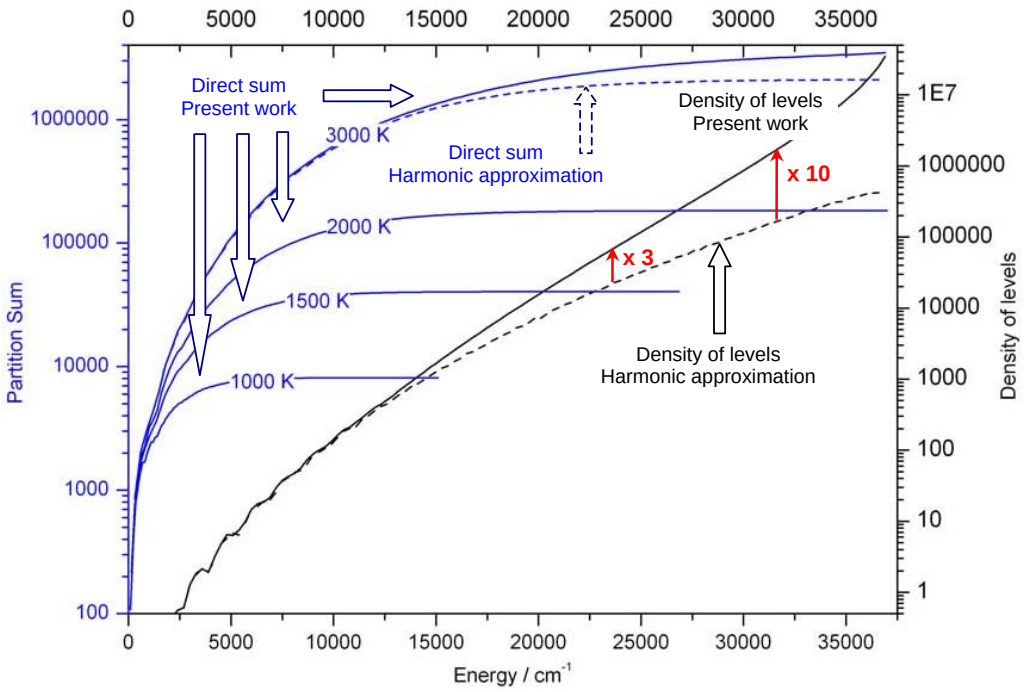

Figure 3: Right part : Density of rovibrational levels predicted using the present work (plain line) and using the harmonic approximation (dashed line). The discrepancies between the densities of levels predicted using the harmonic approximation and the present modelling reach a factor three around 23 000 cm^{-1} and ten around 32 000 cm^{-1} (red arrows). Left part : Partition functions for typical high temperatures showing the convergence properties of the partition direct sums.

uncertainties (less than 1%) are significantly smaller than the observed discrepancies. For higher temperatures our estimated uncertainties become relatively large. Although more realistic than the previous ones our very high temperature values need to be confirmed.

5 Conclusion

A multi-resolution approach has been applied to the direct calculation of the partition function of methane to get more reliable values up to 3000 K. In connexion with the STDS package [14], a computer code has been written and installed on the web at http://icb.u-bourgogne.fr/JSP/TIPS.jsp to be executed on line. Precision estimates as well as detailed information on the density of levels and states of methane are provided as indicators of the reliability of the results. The main conclusions of the present work may be summarized as follows : (i) we have confirmed the validity domain (below 1000 K) of the harmonic approximation as formulated by the original work of McDowell [6] using an independent alternative approach ; (ii) we have quantified the biais resulting from the simple extrapolation of McDowell formula above 1000 K as implemented in the HITRAN database [7] ; (iii) we have proposed alternative partition fonction values for high temperatures by taking into account anharmonicity effects based on the present state of the art of the modelling of the energy spectrum of the methane molecule. The present approach can be adapted to other molecular species having a similar polyad structure and firstly to the isotopomers $^{13}CH_4$, $^{12}CH_3D$. The extension of such a multi-resolution approach to model the absorption coefficient of methane is under study for high temperature applications in parallel with line by line global analyses in progress.

Acknowledgments

Support from the Région Bourgogne for the computer equipment of the Institut Carnot de Bourgogne is gratefully acknowledged.

Table 4: Partition sum of methane (Present versus HITRAN 2004)

	Present work			HITRAN 2004 [7]	HITRAN − Present
Temp. /K	Value	Uncertainty	Equiv. ΔT	(parsum.dat)	Percent
100	116.4	< 0.1 %	< 0.1	116.415997	0.01 %
200	326.6	< 0.1 %	< 0.1	326.631038	0.00 %
300	602.8	< 0.1 %	< 0.1	602.783207	-0.01 %
400	954.7	< 0.1 %	< 0.1	954.176097	-0.05 %
500	1417.7	< 0.1 %	< 0.1	1415.863977	-0.13 %
600	2045.7	< 0.1 %	< 0.1	2040.847920	-0.25 %
700	2910.7	< 0.1 %	< 0.1	2899.589576	-0.40 %
800	4109.1	< 0.1 %	< 0.1	4085.949715	-0.58 %
900	5770.1	< 0.1 %	< 0.1	5724.910637	-0.81 %
1000	8067.4	< 0.1 %	< 0.1	7983.128758	-1.1 %
1100	1.1233×10^4	< 0.1 %	< 0.1	11081.084249	-1.4 %
1200	1.5576×10^4	< 0.1 %	< 0.1	15311.088000	-1.7 %
1300	2.151×10^4	< 0.1 %	< 0.1	21053.744000	-2.2 %
1400	2.960×10^4	0.1 %	< 0.1	28801.928000	-2.7 %
1500	4.058×10^4	0.1 %	< 0.1	39195.464000	-3.5 %
1600	5.550×10^4	0.2 %	< 0.1	53049.504000	-4.4 %
1700	7.569×10^4	0.3 %	< 0.1	71405.104000	-5.7 %
1800	1.031×10^5	0.4 %	0.2	95576.712000	-7.4 %
1900	1.404×10^5	0.6 %	0.4	127212.960000	-9.4 %
2000	1.91×10^5	0.9 %	0.8	168386.400000	-12 %
2100	2.60×10^5	1.2 %	1.7	221649.840000	-15 %
2200	3.54×10^5	1.7 %	3.5	290181.040000	-18 %
2300	4.82×10^5	2.3 %	7	377872.080000	-22 %
2400	6.58×10^5	3.0 %	12	489486.880000	-26 %
2500	8.97×10^5	3.8 %	20	630824.480000	-30 %
2600	1.22×10^6	4.8 %	30	808914.880000	-34 %
2700	1.67×10^6	5.7 %	50	1032217.520000	-38 %
2800	2.27×10^6	6.7 %	65	1311021.600000	-42 %
2900	3.09×10^6	7.5 %	80	1657300.800000	-46 %
3000	4.19×10^6	8.3 %	120	2085888.000000	-50 %

References

[1] Wiedemann G, Deming D, Bjoraker G. A sensitive search for methane in the infrared spectrum of tau bootis. Astrophysical Journal 2001;546:1068–1074.

[2] Sengupta S , Krishan V. Line formation in the atmosphere of brown dwarf gliese 229b: CH_4 at 2.3 μ m. Astronomy and Astrophysics 2000;358:L33–L36.

[3] Swain MR, Vasisht G, Tinetti G. The presence of methane in the atmosphere of an extrasolar planet. Nature 2008;452:329–331.

[4] Goldman A, Gamache RR, Perrin A, Flaud JM, Rinsland CP, Rothman LS. Hitran partition functions and weighted transition-moments squared. Journal of Quantitative Spectroscopy and Radiative Transfer 2000;66:455–486.

[5] Fischer J, Gamache RR, Goldman A, Rothman LS, Perrin A. Total internal partition sums for molecular species in the 2000 edition of the hitran database. Journal of Quantitative Spectroscopy and Radiative Transfer 2003;82:401–412.

[6] McDowell RS. Rotational partition-functions for spherical-top molecules. Journal of Quantitative Spectroscopy and Radiative Transfer 1987;38:337–346.

[7] Rothman LS, Jacquemart D, Barbe A, Benner DC, Birk M, Brown LR, Carleer MR, Chackerian C, Chance K, Coudert LH, Dana V, Devi VM, Flaud JM, Gamache RR, Goldman A, Hartmann JM, Jucks KW, Maki AG, Mandin JY, Massie ST, Orphal J, Perrin A, Rinsland CP, Smith MAH, Tennyson J, Tolchenov RN,

Toth RA, Vander Auwera J, Varanasi P, Wagner G. The hitran 2004 molecular spectroscopic database. Journal of Quantitative Spectroscopy and Radiative Transfer 2005;96:139–204.

[8] Chakraborty A, Truhlar DG, Bowman JM, Carter S. Calculation of converged rovibrational energies and partition function for methane using vibrational-rotational configuration interaction. Journal of Chemical Physics 2004;121:2071–2084.

[9] Thievin J, Georges R, Carles S, Abdessamad B, Rowe B, Champion JP. High temperature emission spectroscopy of methane. Journal of Quantitative Spectroscopy and Radiative Transfer 2008;109:2027–2036.

[10] Champion JP, Loete M, Pierre G. Spherical top spectra. In: Rao K, Weber A, editors. Spectroscopy of the Earth's atmosphere and interstellar medium, Columbus, Academic Press Inc., 1992, p. 339–422.

[11] Boudon V, Champion JP, Gabard T, Loete M, Michelot F, Pierre G, Rotger M, Wenger C, Rey M. Symmetry-adapted tensorial formalism to model rovibrational and rovibronic spectra of molecules pertaining to various point groups. Journal of Molecular Spectroscopy 2004;228:620–634.

[12] Champion JP. Développement complet de l'hamiltonien de vibration-rotation adapté à l'étude des interactions dans les molécules toupies sphériques. application aux bandes ν_2 et ν_4 de $^{12}CH_4$. Canadian Journal of Physics 1977;55:1802–1828.

[13] Berger H. Classification of energy levels for polyatomic molecules. Journal de physique 1977;38:1371–1375.

[14] Wenger C, Champion JP. STDS spherical top data system. A software for the simulation of spherical top spectra. Journal of Quantitative Spectroscopy and Radiative Transfer 1998;59:471–480.

[15] Nikitin A, Boudon V, Champion JP, Albert S, Bauerecker S, Quack M, Brown LR. Global frequency and infrared intensity analysis of $^{12}CH_4$ lines in the 900-4800 cm^{-1} region. 61th International Symposium on Molecular Spectroscopy, Columbus OHIO 2006; http://hdl.handle.net/1811/30962 and paper to appear.

[16] Borysov A, Champion JP, Jorgensen UG, Wenger C. Towards simulation of high temperature methane spectra. Molecular Physics 2002;100:3585–3594.

[17] Bancewicz M. The derivation of the characteristic function and the spectral density distribution of a hamiltonian of n-coupled morse oscillators. International Journal of Quantum Chemistry 2005;102:31–37.

[18] Gribov LA, Novakov IA, A. Pavlyuchko AI, Shumovskii OY. Spectroscopic calculation of the bond-dissociation energy of ch bonds in fluoro derivatives of methane, ethane, ethene, propene, and benzene. Journal of Structural Chemistry 2007;48:400–406.

[19] Sadovskii DA, Zhilinskii BI. Counting levels within vibrational polyads: Generating function approach. Journal of Chemical Physics 1995;103:10520–10536.